Received: 16 May 2020 | Revised: 17 December 2020 | Accepted: 7 February 2021

DOI: 10.1002/joc.7058

RESEARCH ARTICLE

International Journal of Climatology RMetS

Spatiotemporal patterns of ENSO-precipitation relationships in the tropical Andes of southern Peru and Bolivia

Joseph A. Jonaitis[1] | **L. Baker Perry**[1] | **Peter T. Soulé**[1] | **Christopher Thaxton**[2] | **Marcos F. Andrade-Flores**[3,4] | **Tania Ita Vargas**[1] | **Laura Ticona**[3]

[1]Department of Geography and Planning, Appalachian State University, Boone, North Carolina

[2]Department of Physics and Astronomy, Appalachian State University, Boone, North Carolina

[3]Laboratorio de Física de la Atmósfera, Instituto de Investigaciones Físicas, Universidad Mayor de San Andrés, La Paz, Bolivia

[4]Department of Atmospheric and Oceanic Science, University of Maryland, College Park, Maryland

Correspondence
L. Baker Perry, Department of Geography and Planning, Appalachian State University, Boone, NC.
Email: perrylb@appstate.edu

Funding information
National Science Foundation, Grant/Award Number: AGS-1347179

Abstract

Precipitation in the outer tropical Andes is highly seasonal, exhibits considerable interannual variability, and is vital for regulating freshwater availability, flooding, glacier mass balance, and droughts. The primary driver of interannual variability is El Niño Southern Oscillation (ENSO), with most investigations reporting that the El Niño (La Niña) results in negative (positive) precipitation anomalies across the region. Recent investigations, however, have identified substantial spatiotemporal differences in ENSO-precipitation relationships. Motivated by the dissimilarity of these findings, this study examines a carefully selected data set (≥ 90% completeness) of ground-based precipitation observations from 75 high-elevation (≥ 2,500 m above sea level) meteorological stations in the tropical Andes of southern Peru and Bolivia for the period 1972–2016. Distinct groups of stations and associated variability in precipitation characteristics (e.g., total seasonal precipitation, wet season onset, and wet season length) are identified. Using no spatial constraints, the K-Means algorithm optimally grouped stations into five easily identifiable groups. The groups farthest from the Amazon basin had significant negative (positive) precipitation anomalies ($p < .05$) during El Niño (La Niña), aligning with the traditional view of ENSO-precipitation relationships while groups closest to the Amazon had opposite relationships. Additionally, though studies have reported delays in the wet season, years characterized by El Niño had an earlier wet season onset in all five groups. These findings may aid in improving seasonal climate prediction and managing water resources, and could allow for improved interpretation of tropical Andean ice cores.

KEYWORDS

Bolivia, ENSO, Peru, precipitation, tropical Andes

1 | INTRODUCTION

The Andes Mountains, the longest continental mountain range in the world, contains some of the world's most diverse habitats and 99% of all the tropical glaciers in the world, with Peru and Bolivia claiming 71 and 20%, respectively (Francou and Vincent, 2007; Rabatel *et al*., 2012). Glaciers store thousands of years of climate records (Thompson *et al*., 1986; Ramirez *et al*., 2003; Haines *et al*., 2016) and help regulate regional natural hazards such as landslides, floods, droughts, and water shortages in this region (Anderson *et al*., 2017; Vuille *et al*., 2017). Andean glacier mass balance is highly negative at present (Rabatel *et al*., 2012; López-Moreno *et al*., 2014; Veettil *et al*., 2018) and predicted warming of 5–6°C by the end of the century (Urrutia and Vuille, 2009) in this region could mean the disappearance of all glaciers below 5,400 m above sea level (asl; omitted hereafter), ∼50% of all glaciers in the area (Soruco *et al*., 2009).

Primary mechanisms for glacial loss in the outer tropical Andes of southern Peru and Bolivia, a region between 12 and 18°S which contains part of the Altiplano, include increasing temperatures (Ramirez *et al*., 2001; Bradley *et al*., 2006), variable precipitation, and possible reduction in cloud cover (Francou *et al*., 2003; Favier *et al*., 2004). Glaciers in the outer tropics are more sensitive to perturbations in precipitation compared with the inner tropics (Maussion *et al*., 2015), although there are numerous challenges to studying precipitation across the region including spatially complex precipitation patterns (Aalto *et al*., 2003; Ronchail and Gallaire, 2006), scarce observations, and high topographic relief ranging from sea level to 6,542 m.

The El Niño-Southern Oscillation (ENSO) determines the majority of inter-annual precipitation variability in the outer tropical Andes (Francou and Pizarro, 1985, Vuille *et al*., 2000, Garreaud and Aceituno, 2001, Imfeld *et al*., 2021). Most research (e.g., Vuille *et al*., 2000; Garreaud and Aceituno, 2001; Ronchail and Gallaire, 2006; Rabatel *et al*., 2012) reveals negative precipitation anomalies occurring during the warm phase (El Niño) and positive anomalies during the cold phase (La Niña), respectively. Precipitation responses to ENSO phases have been found to reverse over time in the outer tropical Andes (Aalto *et al*., 2003) and vary in regions adjacent to the study area (Ronchail and Gallaire, 2006) (Figure 1). Some studies (Perry *et al*., 2014; Perry *et al*., 2017; Sulca *et al*., 2018) characterizing the ENSO-precipitation relationships in the region have challenged this initial view with ENSO phases associated with opposing precipitation anomalies in some parts of the study area.

To resolve the differences among these studies, the present study investigates the subregional variability of ENSO-precipitation relationships in the outer tropical Andes of southern Peru and Bolivia. In order to identify ENSO-precipitation relationships in this intermontane region, this investigation examines gauge-based precipitation data from

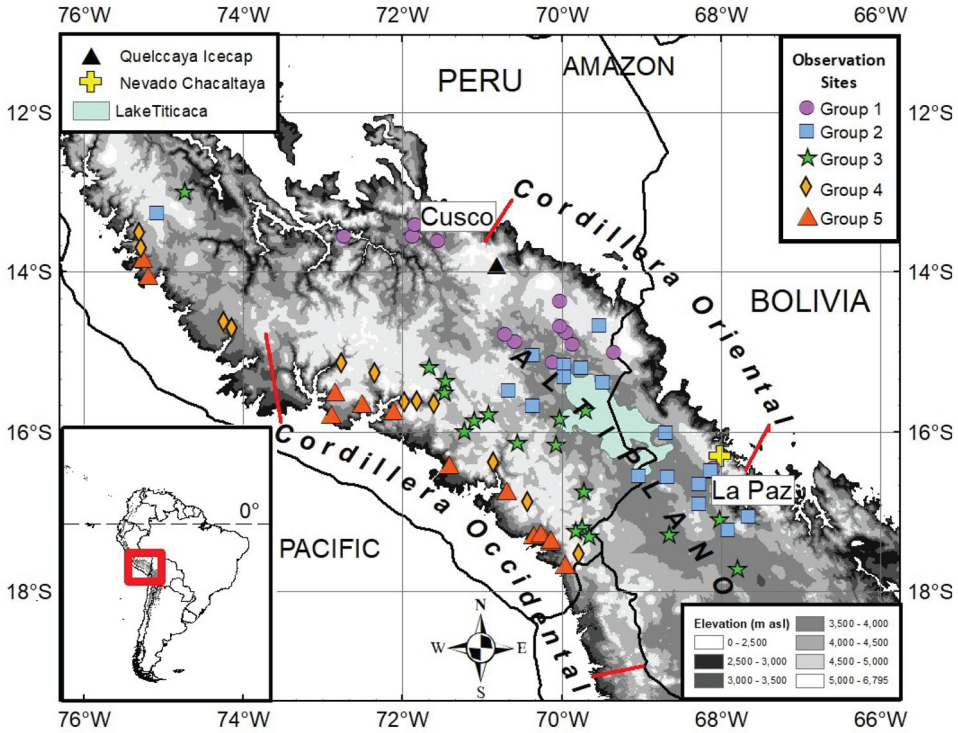

FIGURE 1 Map of study region with the 75 observation sites above 2,500 m that had 90% or more completeness in precipitation observations from 1972 to 2016. The sites were grouped into five groups by average wet season onset over 1972 to 2016 using the K-means grouping method in ArcMap 10.4.1. Red lines indicate approximate extent of the cordillera occidental and cordillera oriental

selected high elevation sites (≥ 2,500 m) that have near-complete (≥ 90%) precipitation records over a 45-year period (Figure 1). The study region is divided into optimally selected groups in order to investigate the intraregional variability of precipitation (e.g., Eck *et al*., 2017). The distinct patterns identified by these new analyses help to resolve disparities among previous studies and may provide critical information to scientists and local stakeholders to improve scientific understanding of ENSO-precipitation relationships in the outer tropical Andes.

2 | LITERATURE SYNTHESIS

Precipitation in the outer tropical Andes has distinct seasons, with a single wet season typically extending from October to March (Perry *et al*., 2017; Andrade *et al*., 2018). Seasonal precipitation totals increase over the study region from the southwest to the northeast, and over 50% of precipitation occurs during the austral summer from December to February (Garreaud and Aceituno, 2001; Perry *et al*., 2014). Precipitation during the wet season results from the release of latent heat associated with Amazon monsoonal convection and is marked by the formation of the Bolivian High and Chaco Low at upper and lower levels of the atmosphere, respectively (Figueroa *et al*., 1995, Lenters and Cook 1999, Rodwell and Hoskins, 2001, Seluchi *et al*., 2003). The northern branch of the Bolivian High is associated with upper-level (300–200 hPa) easterly winds, which are also associated with mid-level moisture transport from the Amazon and convection in the Andes (Garreaud, 1999). The wet season in the region is characterized by northerly and easterly flow at lower levels. Conversely, westerly winds at the middle and upper levels with low specific humidity dominate the dry season, and are associated with a near-complete dissipation of the Bolivian high (Vuille *et al*., 1998; Garreaud *et al*., 2003). In the intermontane region, pluvial periods lasting one to 2 weeks alternate with dry periods of equal length (Garreaud and Aceituno, 2001; Guy *et al*., 2019). This episodic pattern is regionally coherent (Garreaud, 2000; Perry *et al*., 2014) and likely linked with the South American Low-Level Jet (SALLJ) (Guy *et al*., 2019) or cross-equatorial wind variability in the lower troposphere (Espinoza *et al*., 2015), both of which influence moisture provision from the Amazon lowlands to the Andes. At daily time scales, precipitation in the outer tropical Andes occurs predominantly as convective events during the afternoon and longer-lasting stratiform events during the night-time (Perry *et al*., 2014; Chavez and Takahashi, 2017; Junquas *et al*., 2018).

The Amazon Basin is the source of about 95% of the moisture for precipitating events in the region, as inferred from backward air trajectories in Cusco and La Paz (Perry *et al*., 2014). Moisture transport is primarily light around 1–3 $m \cdot s^{-1}$ (Vimeux *et al*., 2005, Perry *et al*., 2014), is parallel with and enhanced by the SALLJ (Junquas *et al*., 2018), and originates from the west and north of the region (Ronchail and Gallaire, 2006; Perry *et al*., 2014). Though seemingly contradictory, northwesterly moist flow in southern Peru still advects moisture from the Amazon basin due to regional topography. Over the Bolivian Altiplano, precipitation decreases occur from east to west and north to south as moisture is uplifted while crossing the Andes (Ronchail and Gallaire, 2006). Valleys that cut across the Andes and orient with the SALLJ from northwest to southeast channel the moisture to the region (Junquas *et al*., 2018).

Contributing to the majority of interannual precipitation variability in the region (Francou and Pizarro, 1985; Vuille *et al*., 2000; Garreaud and Aceituno, 2001), ENSO is a complex teleconnection pattern with distinct signals throughout the world (Philander, 1983; Trenberth, 1997). Many investigations (e.g., Aceituno, 1988; Vuille, 1999; Vuille *et al*., 2000; Garreaud and Aceituno, 2001; Ronchail and Gallaire, 2006; Rabatel *et al*., 2012) have found that El Niño correlates with negative precipitation anomalies and La Niña correlates with positive precipitation anomalies in the outer tropical Andes and in the Cordillera Blanca of Peru (Maussion *et al*., 2015). In the upper 59.2 m of an ice core from Nevado Illimani (Bolivia), increased dust correlated with decreased annual layer ice thickness and El Niño; decreased dust correlated with increased annual layer thickness and La Niña (Knüsel *et al*., 2005). Since glacial mass balance depends on the inter-annual variability of precipitation (Favier *et al*., 2004), Veettil *et al*. (2016) concluded that rises in snowline altitude (SLA) corresponded with decreases in precipitation. Selected glaciers in the Cordillera Occidental and the Cordillera Oriental tended to have higher SLAs during El Niño and lower SLAs during La Niña (Veettil *et al*., 2016, 2018). Furthermore, when the warm phase of PDO and El Niño and the cold phase of PDO and La Niña aligned, the effects of El Niño and La Niña were stronger on SLA. Increased glacial runoff from the Zongo glacier 30 km north of La Paz was also associated with El Niño when compared with runoff during ENSO Neutral (i.e., neither El Niño or La Niña) years (Ribstein *et al*., 1995). The amount of precipitation attributed to the runoff decreased when compared with ENSO Neutral phase years, suggesting negative precipitation anomalies during El Niño and enhanced melt when compared with ENSO Neutral phase years (Ribstein *et al*., 1995).

Recent attempts to characterize ENSO-precipitation relationships using ground-based precipitation data in the outer tropical Andes show conflicting results. Perry *et al*. (2014) found that portions of the Cordillera Oriental near Cusco had negative precipitation anomalies during

TABLE 1 Summary of data sets used

Data type	Temporal resolution	Period	Source
1. **Precipitation SENAMHI sites of Bolivia (12)**	Daily	1972–2017	DECADE project and SENAMHI Bolivia
SENAMHI sites of Peru (63)	Daily	1972–2018	SENAMHI Peru
2. **Teleconnection pattern indices** **Multivariate ENSO index (MEI)**	Monthly	1871–2018	U.S. Earth System Research Lab, NOAA

the 2007–2008 La Niña and positive precipitation anomalies during the subsequent 2009–2010 El Niño. In an additional study (Perry *et al*., 2017), La Paz exhibited negative precipitation anomalies during both phases of ENSO from 1979 to 2009, whereas Cusco exhibited positive precipitation anomalies during El Niño and negative anomalies during La Niña from 1963 to 2009 (Perry *et al*., 2014; Perry *et al*., 2017). In the Mantaro River Basin of Peru, El Niño favours a late onset and early end to the wet season whereas an early onset and late end with La Niña (Giráldez *et al*., 2020). ENSO variability may also be influencing long-term trends in precipitation across the region (Heidinger *et al*., 2018).

Further illustrating the complexity of the effect of ENSO on the region, Aalto *et al*. (2003) analysed sediment cores near rivers in the eastern side of the Cordillera Oriental of northern Bolivia using lead isotopes to determine individual sediment events. They found that rapidly rising floods occurred more frequently during La Niña years. More importantly, they noted that in part of the floodplain, the response to ENSO flipped in the early 1970s—such that rainfall was actually lower during La Niña and sometimes higher during El Niño (Aalto *et al*., 2003). In an additional study (Ronchail and Gallaire, 2006) that examined precipitation observations, ENSO demonstrated distinct relationships on opposite sides of the Cordillera Oriental of northern Bolivia. Whereas the western side of the cordillera and the Altiplano of Bolivia recorded negative precipitation anomalies during El Niño and positive precipitation anomalies during La Niña, the opposite precipitation anomalies occurred on the eastern side of the cordillera (Ronchail and Gallaire, 2006). Location and timing seemed to play a crucial role on how the ENSO-precipitation relationship is expressed, even within regions of Bolivia.

The primary research question we address in this study is: how do precipitation characteristics vary across space and through time as a function of ENSO phase over the study area? The analyses are based on daily precipitation observations from 75 high-elevation sites (≥ 2,500 m) in the Andes of southern Peru and Bolivia with near-complete precipitation records (≥ 90%) over a 45-year period. This work is motivated by the identified need to improve scientific understanding of ENSO-precipitation relationships in space and time, and the desire to provide better guidance to stakeholders in the region who need to plan for a changing climate.

3 | DATA AND METHODS

3.1 | Study area and data sets

The Peruvian National Meteorology and Hydrology Service (SENAMHI), Bolivian SENAMHI, and the project Data on Climate and Extreme Weather for the Central Andes (DECADE) (Andrade *et al*., 2018; Hunziker *et al*., 2018) provided daily precipitation observations from stations between 12.5 and 18°S in southern Peru and Bolivia (Table 1). The precipitation observations, which originated from 533 Peruvian SENAMHI and 241 Bolivian SENAMHI manual and automatic stations, spanned from 1931 to the present and from 1917 to the present, respectively. In order to focus on the north central Altiplano and its bordering areas, the study region only included stations ≥2,500 m. This study only used stations with 90% completeness in their data set, surpassing the minimum recommended completeness for climate normals (80%) (WMO 2011). The analysis extends from July 1, 1972 to June 30, 2017 (hereafter referred to as years 1972–2016 or simply 1972–2016) because the period includes the greatest number of stations (75) at 90% completeness over the longest time series including multiple El Niño and La Niña events.

3.2 | Computation of precipitation characteristics

The daily precipitation observations provided the foundation for determining a set of eight climatological characteristics, namely: total annual (July 1–June 30) precipitation, total wet season precipitation, wet season onset, dry season onset, wet season length, peak wet season date, number of wet days, and number of very wet days for each observation

site. Liebmann *et al*. (2007) detailed the method for computing the wet and dry season onset used to derive the wet season length and total wet season precipitation. A station that recorded measurable precipitation (>0) during a calendar day signified one wet day. Trace precipitation, which is a small amount of precipitation (< 0.2 mm) that is difficult to measure, is set to zero on these data sets. A very wet day was counted when a station recorded precipitation during a calendar day that was at or above the 95th percentile of all precipitation observations during the entire study period.

3.3 | Grouping analysis

The K-Means algorithm (Hartigan and Wong, 1979), a grouping analysis tool in ESRI's ArcMap 10.4.1, grouped stations by their precipitation characteristics without employing spatial constraints. The tool constructed different groups by first finding the stations that had the greatest differences in a characteristic—called 'starting' stations—and then grouped other stations with similar characteristics with those starting stations. The station characteristics used to group the stations included all the aforementioned precipitation characteristics, geographical properties of the station such as latitude and elevation, and combinations of all of these characteristics. Multiple grouping analyses were performed, testing how well different station characteristics grouped stations. An R^2 value and a Calinski-Harabasz pseudo-F-statistic (F) (Caliński and Harabasz, 1974) assessed both the fitness of the precipitation characteristic(s) used and the groups developed. The closer an R^2 value was to 1.0, the better the precipitation characteristic was for discriminating among the groups. This study sought groups of stations with R^2 values over .95. Two to 15 hypothetical groups were produced for each grouping analysis. Each set of groups produced an F that reflected within-group similarity and between-group differences. The optimal number of groups demonstrated the highest F value while also maintaining the lowest number of groups.

3.4 | Identifying ENSO-precipitation relationships

Eight precipitation characteristics were computed for the overall study region and each group during each year from 1972 to 2016. In addition to these characteristics, the coefficient of variation (CV) was computed for total wet season precipitation. Following Climate Prediction Center (2018) protocol, each year was categorized as an El Niño or La Niña year if five or more consecutive bi-monthly index values from the Multivariate ENSO Index (MEI) (Earth System Research Lab) were greater than 0.5 or less than −0.5, respectively. Any years not identified as El Niño or La Niña were categorized as ENSO Neutral years. The Kruskal-Wallis H (Kruskal and Wallis, 1952) test revealed if any ENSO phase exhibited significant differences in the precipitation characteristics. A post hoc Kruskal-Wallis H test (Dunn, 1964), which employs a Bonferroni correction for multiple tests (Bonferroni, 1936), was used to complete a pairwise comparison of all ENSO phases to reveal which ENSO phase pairs had significant differences. Unless otherwise noted, all differences reported were significant at the 0.05 level. For further validation, the Spearman's rank-order correlation tested the strength and direction between various groupings of MEI values and the precipitation characteristics.

4 | RESULTS

4.1 | Groups and their precipitation characteristics

Average wet season onset grouped the 75 stations in the study area most effectively (Figure 1). The grouping analysis produced four and five station groups with R^2 values of .97 and .97, respectively. These two groupings represented the minimum number of station groups that produced R^2 values over .95. Groupings with more than five station groups were not considered even if they had R^2 values over .95. The F also had increased values when stations were divided into four or five groups when compared with fewer groups. Multiple iterations of the grouping analysis revealed that F values remained relatively constant when grouping stations into five groups but had substantial drops when grouping stations into four groups. Thus, five groups were selected for further analysis.

The five groups were numbered from 1 to 5, and ordered from earliest to the latest wet season onset date (Figure 2a), following a NW to SE orientation. Group 1 incorporated the eastern Peruvian highlands, Quelccaya Ice Cap, and Cusco, while Group 2 incorporated most of Lake Titicaca, the northeastern Bolivian highlands, La Paz, and Mount Chacaltaya. Median station elevation for Groups 1 and 2 were 3,903 and 3,840 m, respectively (Figure 2b). Groups 3, 4, and 5 were in the western cordillera and highlands of Peru and Bolivia with a median station elevation of 3,872, 3,367, and 3,214 m, respectively. Groups 3, 4, and 5, which were the closest to the Pacific coast, demonstrated the latest average wet season onsets (December 7, 15, and 29, respectively), and Groups 1 and 2, closest to the Amazon Basin, had the earliest wet season onset (November 11, and 20, respectively).

Precipitation was highest in Groups 1 and 2 with 569 and 516 mm average wet season precipitation (Table 2) and 686 and 641 mm average annual precipitation, respectively (Figure 2c). Groups 3, 4, and 5 followed regional patterns receiving 500, 398, and 219 mm on

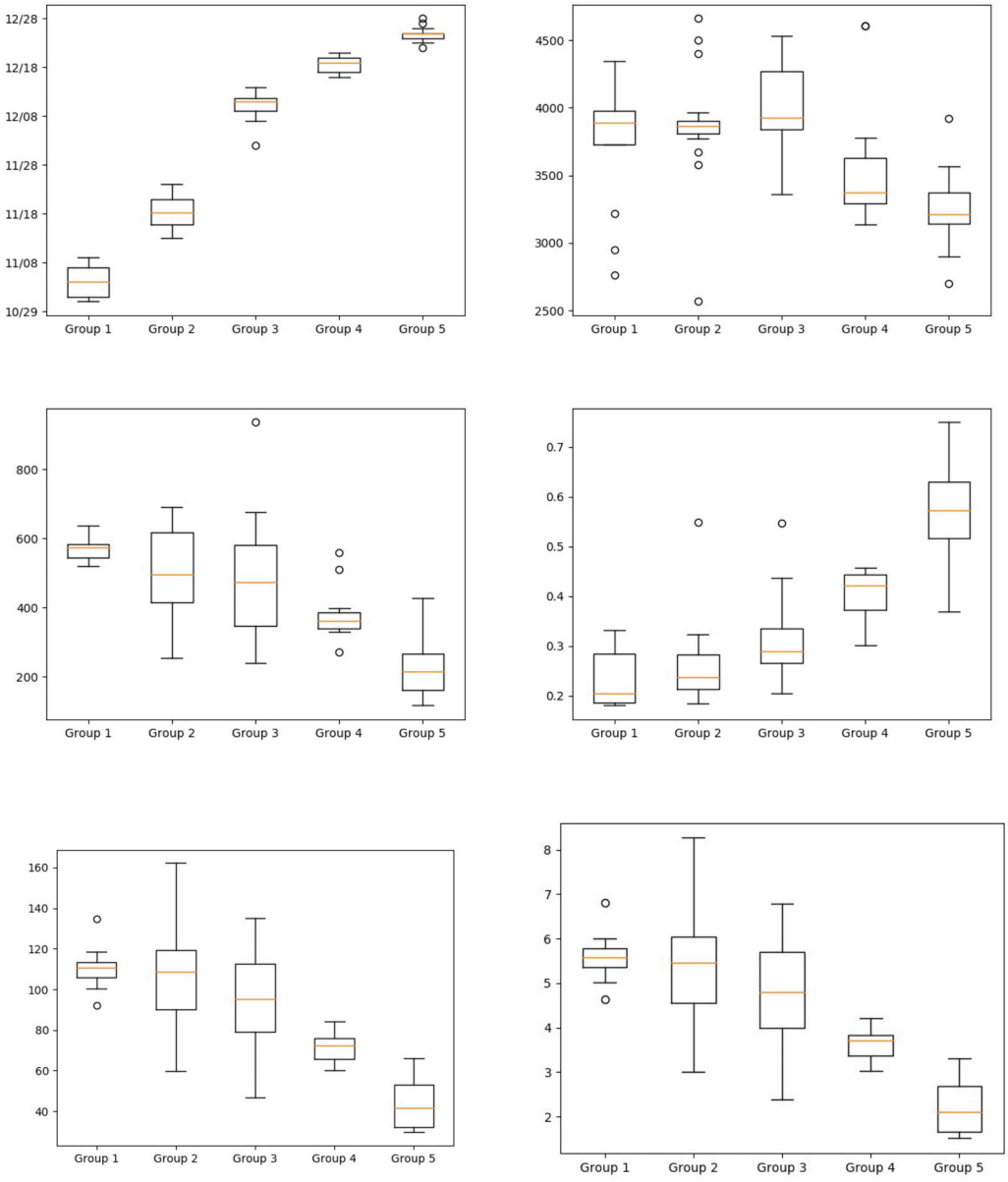

FIGURE 2 Box and whisker plots displaying minimum, first quartile, median, third quartile, and maximum wet season onset (month/day) (a), elevation (m) (b), total wet season precipitation (mm) (c), coefficient of variation of total wet season precipitation (d), wet days (e), and very wet days (≥ 95th percentile) (f) of the 75 observations sites according to group

TABLE 2 Average total wet season precipitation (mm) of all observation stations and the *SD* within the entire study region (all) and within Groups 1–5 averaged over the years from 1972 to 2016 (mean) and averaged over only El Niño, La Niña, and ENSO neutral years from that same period

Group	Mean	*SD*	El Niño	La Niña	Neutral	LN-EN diff	NE-LN diff	EN-NE diff
1	569	91	564	524	601	−40	77	−37
2	516	94	497	477	559	−20	82	−62
3	500	114	447	528	541	81	13	−94
4	398	118	341	476	413	135	−63	−72
5	219	102	169	302	224	133	−78	−55
All	450	84	414	464	480	50	16	−66

Note: Differences between La Niña (LN), El Niño (EN), and ENSO neutral years (NE) are also reported.

TABLE 3 Average number of wet days of all observation stations within the entire study region (all) and within Groups 1–5 averaged over the years 1972–2016 (mean) and averaged over only El Niño, La Niña, and ENSO neutral years from that same period

Group	Mean	El Niño	La Niña	Neutral	LN-EN diff	NE-LN diff	EN-NE diff
1	110.5	110.1	111.6	110.4	1.5	−1.2	−0.3
2	107.2	103.1	105.4	112.7	2.3	7.3	−9.5
3	95.7	90.7	98.4	99.4	7.7	1.0	−8.7
4	77.0	69.2	86.9	79.4	17.6	−7.4	−10.2
5	44.3	36.1	58.0	44.9	21.9	−13.0	−8.8
All	88.7	83.7	93.1	91.5	9.4	−1.6	−7.7

Note: Differences between La Niña (LN), El Niño (EN), and ENSO neutral years (NE) are also reported.

TABLE 4 Average wet season onset (month/day) of all observation stations within the entire study region (all) and within Groups 1–5 averaged over the years 1972–2016 (mean) and averaged over only El Niño, La Niña, and ENSO neutral years from that same period

Group	Mean	El Niño	La Niña	Neutral	LN-EN diff	NE-LN diff	EN-NE diff
1	11/11	11/4	11/24	11/11	20	−13	−7
2	11/20	11/10	12/7	11/21	27	−16	−11
3	12/7	12/2	12/13	12/8	11	−5	−6
4	12/15	12/11	12/20	12/16	9	−4	−5
5	12/29	12/26	1/1	12/31	6	−1	−5
All	12/2	11/28	12/9	12/2	11	−7	−4

Note: Differences between La Niña (LN), El Niño (EN), and ENSO neutral years (NE) are also reported.

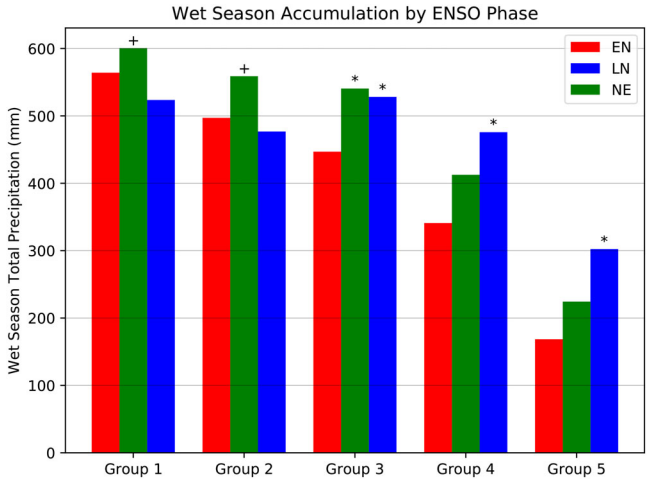

FIGURE 3 Bar graph displaying wet season totals (mm) from 1972 to 2016 for Groups 1–5 averaged by ENSO phase: El Niño (red, $n = 18$), ENSO neutral (green, $n = 17$), and La Niña (blue, $n = 10$). ENSO phases with significantly greater wet season totals than the phase with the lowest wet season total are indicated with a '*' for $p < .05$ or '+' for $p < .1$

average during the wet season (Tables 2 and 3) and 602, 462, and 240 mm on average during the year. The farther south and west the groups were from the Amazon Basin, the less seasonal and annual total precipitation the groups received. The CV, which was lowest and nearly identical in Groups 1 and 2, increased spatially to the south and west coast (Figure 2d). Group 5 had the highest CV indicating that the greatest variability in seasonal precipitation occurred in the west closest to the Pacific coast. The frequency of wet days and very wet days followed precipitation totals; both were the highest in groups nearest the Amazon lowlands in the east and lowest near the coast in the west (Figure 2e,f).

4.2 | Regional and group response to ENSO

The study region as a whole and as individual groups showed statistically significant differences between pairs of different ENSO phases. The overall study region experienced increased total wet season and annual precipitation during ENSO Neutral years (66 and 74 mm more, respectively) compared with El Niño years (Table 2). Although not statistically significant, wet season onset occurred, on average, 11 days earlier during El Niño than during La Niña in the overall study region (Table 4). The dry season onset was also not statistically different among any ENSO phase for any of the groups or the

TABLE 5 Average wet season length (days) of all observation stations within the entire study region (all) and within groups 1–5 averaged over the years 1972–2016 (mean) and averaged over only El Niño, La Niña, and ENSO neutral years from that same period

Group	Mean	El Niño	La Niña	Neutral	LN-EN diff	NE-LN diff	EN-NE diff
1	154.2	160.7	138.7	156.4	−22.0	17.7	4.3
2	139.1	146.1	120.9	142.4	−25.2	21.5	3.7
3	126.0	131.6	117.7	125.1	−13.9	7.4	6.5
4	122.8	127.9	115.0	122.1	−12.9	7.1	5.8
5	95.7	97.3	94.6	94.7	−2.7	0.1	2.6
All	130.9	134.8	122.1	131.9	−12.7	9.8	2.8

Note: Differences between La Niña (LN), El Niño (EN), and ENSO neutral years (NE) are also reported.

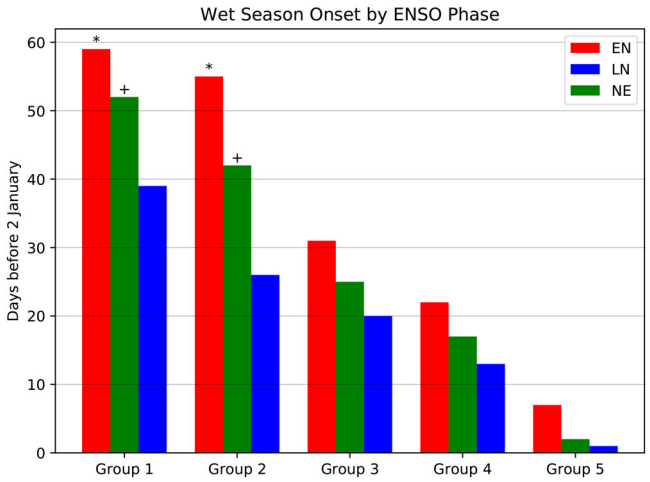

FIGURE 4 Bar graph displaying days before 2 January the wet season began from 1972 to 2016 for Groups 1–5 averaged by ENSO phase: El Niño (red, $n = 18$), ENSO neutral (green, $n = 17$), and La Niña (blue, $n = 10$). ENSO phases with a significantly earlier wet season onset than the phase with the latest wet season onset are indicated with a '*' for $p < .05$ or '+' for $p < .1$

study region as a whole. The average dry season onset occurred on 12 April within the overall study region and within 7 days from that date among all ENSO phases in all the groups.

Groups 1 and 2 exhibited the most precipitation, wet days, and very wet days during El Niño years and the earliest wet season onset in ENSO Neutral years. Both saw an earlier wet season onset (20 and 27 days earlier, respectively) and longer wet season length ($p < .1$ for Group 2 only) during years with El Niño than with La Niña. Group 1 also had 1.3 more very wet days during El Niño years than in La Niña years (Figure 3 and Tables 4 and 5). For both Groups 1 and 2, ENSO Neutral years received the greatest total wet season precipitation (77 and 82 mm, respectively) ($p < .1$) when compared with La Niña years (Figures 4 and 5 and Table 2). Wet season onset occurred 16 days earlier on average in Group 2 during ENSO Neutral years in contrast with La Niña years (Table 5).

Groups 3, 4, and 5 also showed very similar precipitation characteristics in precipitation, number of wet days, and wet season onset. All three groups received increased wet season precipitation (81, 135, and 133 mm more, respectively) during La Niña events when compared with El Niño events (Figures 4 and 5 and Table 2). La Niña years also reported significantly increased total annual precipitation, more wet days, and more very wet days (1.5 and 1.5 days more, respectively) (Table 3) than El Niño years in Groups 4 and 5. ENSO Neutral years showed an increase of 94 mm in total wet season precipitation and 102 mm ($p < .1$) in total annual precipitation when compared with El Niño years in Groups 3 (Figures 4 and 5 and Table 2). La Niña years also experienced positive wet season precipitation anomalies (78 mm) (Table 2) and positive annual precipitation anomalies (85 mm more) than ENSO Neutral years in Group 5.

Spearman's rank-order correlation validated and matched the significant differences found in precipitation characteristics between El Niño and La Niña years for the study region as a whole and individual groups (Table 6). The January–February MEI value correlated best with precipitation in Groups 3, 4, and 5 and the September–October MEI value correlated best with wet season onset in Groups 1 and 2.

5 | DISCUSSION

5.1 | Seasonal and annual precipitation

Differences in positive and negative precipitation anomalies in the study region as a whole and within the individual groups showed similarity with the ENSO-precipitation relationships previously identified for the region. The overall study region received lower annual and wet season

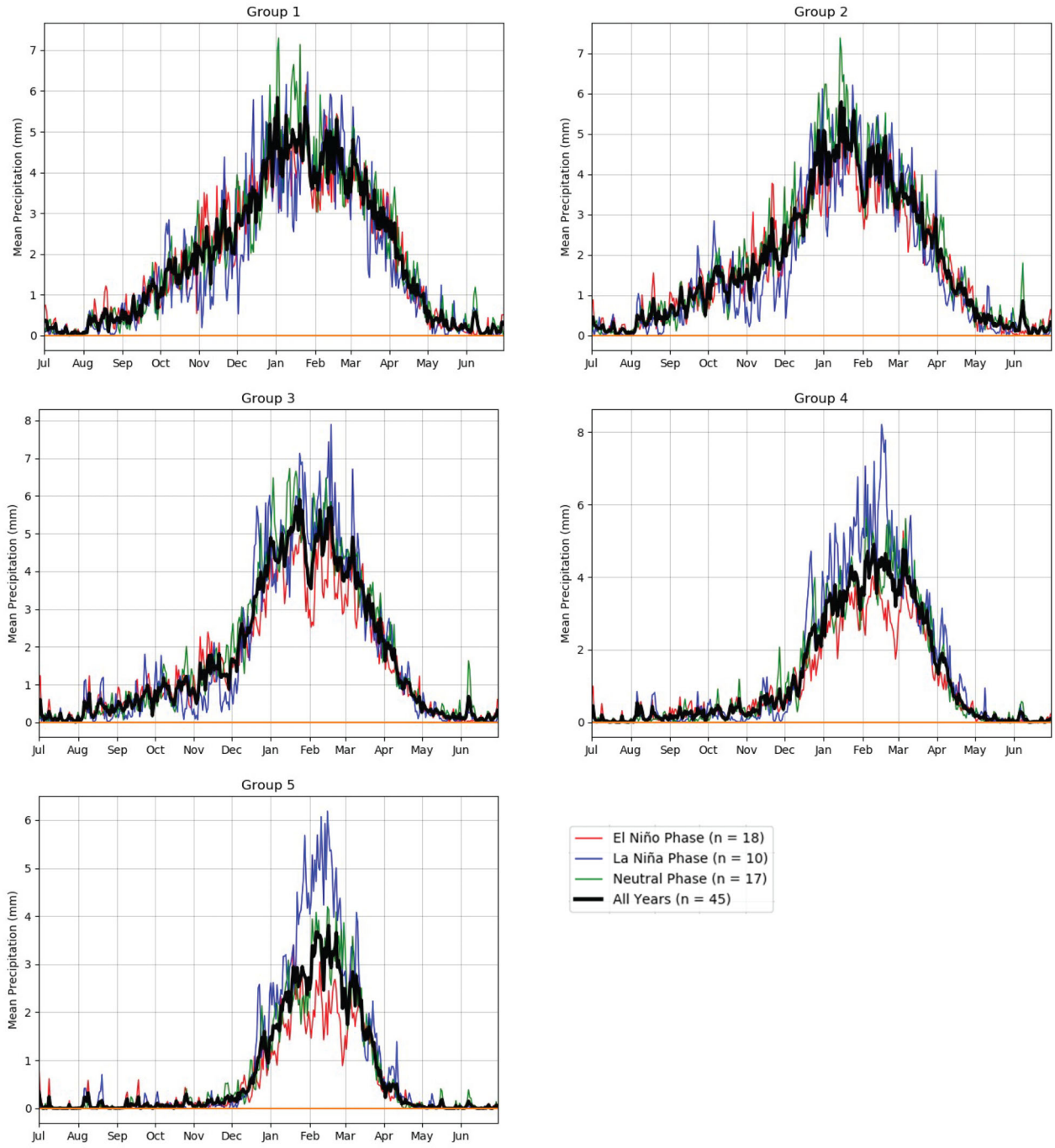

FIGURE 5 Line graph displaying daily mean precipitation (mm) from 1972 to 2016 for Group 1 (a), Group 2 (b), Group 3 (c), Group 4 (d), and Group 5 (e) during El Niño years only (red, $n = 18$), ENSO neutral years only (green, $n = 17$), La Niña years only (blue, $n = 10$), and all years (black, $n = 45$)

precipitation ($p < .1$) during El Niño years, consistent with previous studies (Aceituno, 1988; Vuille, 1999; Vuille *et al.*, 2000; Garreaud and Aceituno, 2001; Ronchail and Gallaire, 2006; Rabatel *et al.*, 2012). Garreaud *et al.* (2003) reported a significant moderate relationship ($r = -.46$) between austral summer precipitation and the Ocean Niño Index (ONI) over the entire Altiplano, consistent with our results between MEI and wet season precipitation over the study area ($r = -.456$, $p < .01$) (Figure 7c and Table 6). Studies (e.g., Garreaud, 1999; Vuille, 1999 and Garreaud *et al.*, 2003) also found that ENSO-precipitation relationships are stronger in the western Altiplano, resulting in El Niño years with greater negative anomalies and La Niña years with greater positive anomalies. Groups 3, 4, and 5, which occupy the western and central parts of the study region, also showed significant positive precipitation

TABLE 6 Spearman's correlation values between annual MEI bimonthly index values and average annual precipitation characteristics within the entire study region (all) and within Groups 1–5: Wet season onset, wet season length, wet season total, annual total, wet days, and very wet days

	September–October					January–February			
Group	Wet season onset	Wet season length	Wet season Total	Wet days	Very wet days	Wet season total	Annual total	Wet days	Very wet days
1	**−0.448****	**0.409****	0.135	−0.096	**0.447****	−0.042	−0.075	−0.126	**0.304***
2	**−0.476****	**0.346***	0.034	−0.116	−0.008	−0.109	−0.116	−0.211	−0.134
3	−0.147	0.213	**−0.412****	−0.284	−0.248	**−0.543****	**−0.495****	**−0.391****	**−0.441****
4	−0.192	0.095	**−0.528****	**−0.427****	**−0.336***	**−0.580****	**−0.532****	**−0.484****	**−0.390****
5	−0.084	−0.050	**−0.501****	**−0.536****	**−0.334***	**−0.604****	**−0.559****	**−0.611****	**−0.448****
All	−0.204	0.230	**−0.338***	−0.289	−0.147	**−0.456****	**−0.443****	**−0.406****	−0.286

Note: Correlations significant at the .05 level and .01 level (2-tailed) are denoted with * and **, respectively.

anomalies in total seasonal precipitation during La Niña events when compared with El Niño events (Figure 3c–e and Table 2). Furthermore, significant inverse relationships between MEI and precipitation became stronger from east to west (from Groups 3 to 5) (Figure 7 and Table 6). Plots of daily mean precipitation for these groups show anomalously positive precipitation in January and February during La Niña years (Figure 5).

Contrary to the traditional ENSO-precipitation understanding (e.g., Vuille *et al*., 2000; Rabatel *et al*., 2012) the behaviour of precipitation is reversed in Groups 1 and 2 in the east of the study region encompassing La Paz, most of Lake Titicaca, Cusco, and the NE half of the north central Altiplano. Although not statistically significant, these groups had on average negative seasonal and yearly total precipitation anomalies during La Niña events and positive precipitation anomalies during El Niño events, although the strong El Niño years exhibited lower precipitation totals (Figure 6). ENSO Neutral years had the highest precipitation totals out of all the ENSO phases. Wet season precipitation totals were significantly greater ($p < .1$) during ENSO Neutral years when compared with La Niña years (Figure 3a,b). In Group 3, ENSO Neutral years also produced more annual and seasonal precipitation than El Niño years, and though not statistically significant, exhibited more precipitation during La Niña years as well. Analysis of daily mean precipitation during each ENSO phase reveals above-average precipitation during ENSO Neutral years particularly in January (Figure 5).

The importance of ENSO Neutral years and the diminished ENSO signal in Groups 1 and 2 still align with the limited studies (e.g., Vuille *et al*., 2000; Garreaud *et al*., 2003; Perry *et al*., 2017) segregating the eastern half of the study region. Eastern areas are largely characterized as having a weak response to ENSO with no relationship between precipitation and ENSO phase (Vuille *et al*., 2000; Garreaud *et al*., 2003). La Paz, for example, experienced negative precipitation anomalies from 1979 to 2009 for both strong El Niño and strong La Niña years (Perry *et al*., 2017).

5.2 | East–West shift in precipitation responses to ENSO

Differences between Groups 1 and 2 with Groups 3, 4, and 5 reveal an east–west ENSO-precipitation dipole that runs along a NW–SE line roughly parallel to the southern border of Lake Titicaca. Because of their similar responses to varying ENSO phases, Groups 1 and 2 will hereafter be referenced as the eastern groups and Groups 3, 4, and 5 as the western groups. One explanation for this divide may lie in differences in moisture availability and transport to these groups during different ENSO phases. Throughout sites in the Altiplano, pluvial episodes occur when mixing ratios exceed 5 $g \cdot kg^{-1}$ and dry episodes occur when below 3 $g \cdot kg^{-1}$ (Garreaud *et al*., 2003). When mixing ratios do exceed 5 $g \cdot kg^{-1}$, deep convection almost invariably results (Garreaud *et al*., 2003).

In general, moisture is advected into the Altiplano from the north and east. Important differences in moisture transport have been found outside the Altiplano in the eastern groups (Vimeux *et al*., 2005; Perry *et al*., 2017; Endries *et al*., 2018). While easterly moist flow still occurred in these groups, 60–70% of precipitation events originated from the north and west near Cusco and La Paz (Perry *et al*., 2017). Furthermore, 83% of 72-hr backward moisture trajectories from 2004 to 2010 in Cusco

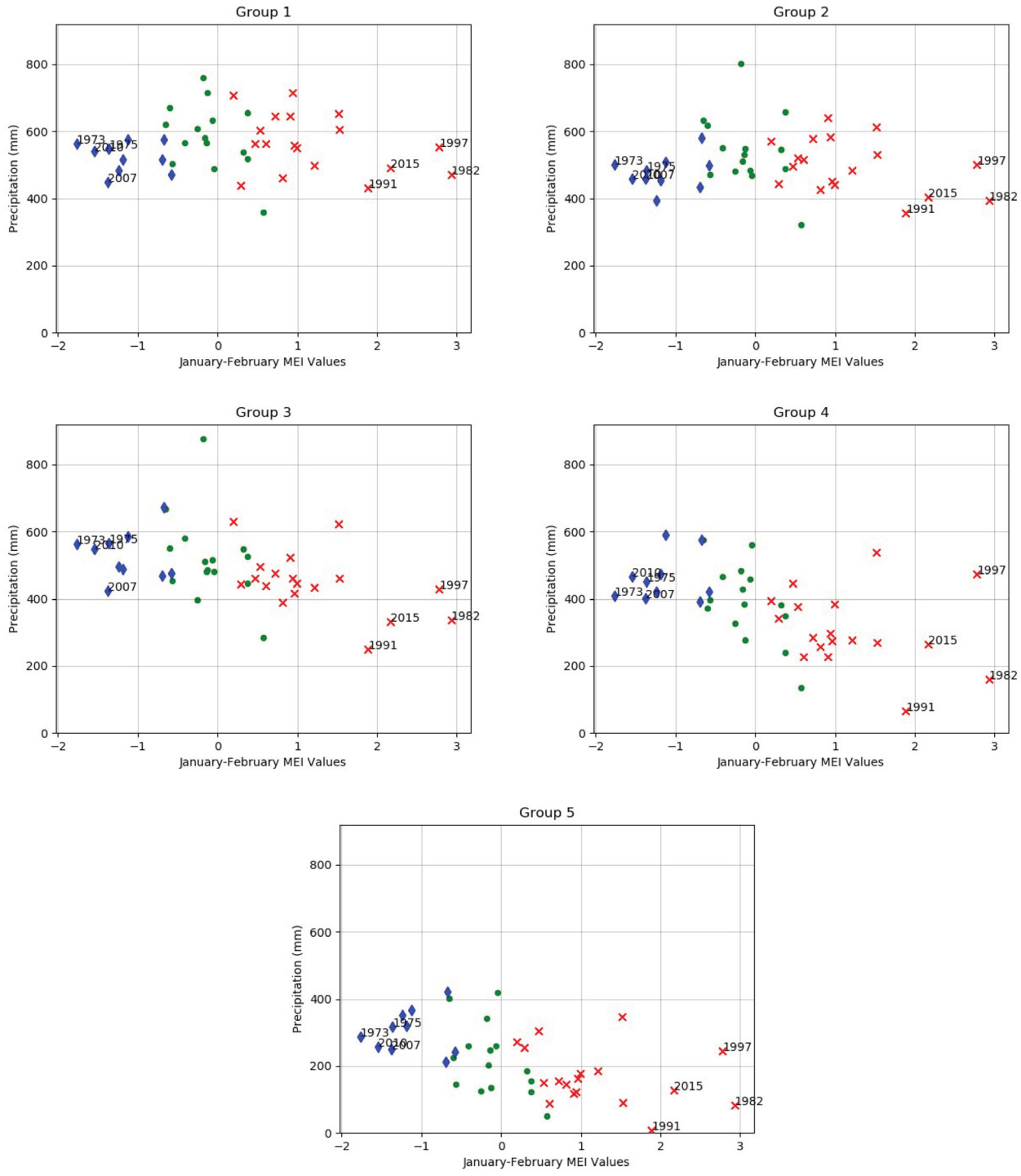

FIGURE 6 Scatterplot displaying January–February MEI values and corresponding wet season total precipitation (mm) for each year from 1972 to 2016 for Group 1 (a), Group 2 (b), Group 3 (c), Group 4 (d), and Group 5 (e). Years classified as El Niño (red x, $n = 18$), ENSO neutral (green circle, $n = 17$), and La Niña (blue diamond, $n = 10$). The strongest four La Niña years (1973, 1975, 2007, and 2010) and El Niño years (1982, 1991, 1997, and 2015) are labelled by the year in which they occurred

originated under weak flow regimes from the NW, NE, and E (Perry *et al*., 2014). The geomorphic configuration of the eastern groups helps explain how northwesterly flow can still provide Amazonian moisture from the northwest since moist continental lowland lies not only to the east and north but to the northwest of areas around Cusco (Figure 1). Northwesterly oriented valleys that cut across the Andes channel moisture to the region

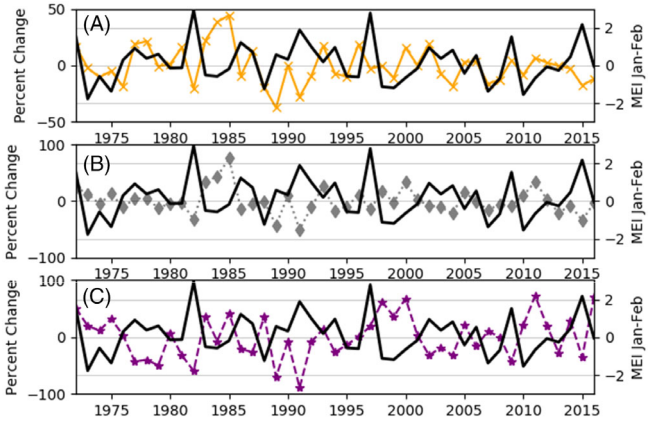

FIGURE 7 Line graph displaying percent change in the wet season total from the mean wet season total from 1972 to 2016 for (a) the average of Groups 1–2, (b) Group 3, and the average of Groups 4–5. January–February MEI values are plotted in black from 1972 to 2016 to provide ENSO phase and strength

in connection with the SALLJ (Junquas *et al*., 2018). For western groups, flow from the northwest would immediately advect from other mountainous regions rather than from the moist continental lowlands (Figure 1).

Differences in moist flow also were noted during varying ENSO phases. The 2007–2008 La Niña exhibited increased moisture advection from the E and NE in Cusco while the 2009–2010 El Niño had increased moisture advection from the NW and NNW (Perry *et al*., 2014). Those findings are consistent with increases in upper and lower level easterlies during La Niña and westerlies during El Niño (Garreaud and Aceituno, 2001). Fluctuations in northwesterly flow during El Niño and La Niña help explain the negative and positive precipitation anomalies. Backward trajectories at high spatial resolution during all ENSO phases in the western groups, however, should be performed for multiple years to test this hypothesis.

Scatterplots of wet season precipitation in the eastern groups and January–February MEI values reveal that positive precipitation anomalies are associated with both ENSO Neutral years and weak El Niño years (Figures 6 and 7). Backward trajectory analyses in eastern groups during specific ENSO phases, including ENSO Neutral, might provide a link as to why weaker ENSO phases favour precipitation in the East.

5.3 | Wet days and very wet days

The more western groups, which may receive the least moisture during El Niño years, recorded fewer wet days (∼16 fewer days collectively on average) during El Niño years than during La Niña years (Table 3). The eastern groups, in contrast, showed inconsistent (if any) changes in the number of wet days during ENSO Neutral years. When compared with La Niña, ENSO Neutral exhibited an increase of 7.3 days in Group 1 and a decrease of 1.2 days in Group 2 even though wet season precipitation during that phase increased by ∼80 mm in both groups.

The hypothesis that moisture availability varies substantially in the east and west of the study region during the same ENSO phase could also explain the differences in wet days and very wet days among the western groups. Increases in moist flow inferred from increases in mean easterly flow in the study area during DJF from 1986 to 1995 resulted in an increase in the number of wet days (Garreaud and Aceituno, 2001). Garreaud and Aceituno (2001) used a 9-day moving average, however, eliminating short-lived episodes that may have coincided with intense events and the ability to detect an increase in the intensity of precipitation with increased moist flow.

5.4 | Wet season onset, dry season onset, and length

Wet season onset is earliest in the northeastern areas of the study region with Groups 1 and 2 having the earliest onsets. Groups to the southwest have wet season onsets that are progressively later in the year. The spatial relationship of wet season onset mirrors the primary direction of moisture delivery from the Amazon (Figure 1 and Table 4) (Garreaud, 1999; Perry *et al*., 2014). During all ENSO phases, moisture to begin the wet season is first delivered to the eastern Groups, on average around the beginning of November. As increased moisture influx occurs in the east, additional moisture is advected further south and west influencing the western groups. Because moisture in Group 5 would need to first pass through all the other groups, Group 5 has the latest wet season onset (January 1). Unlike the wet season onset, the dry season onset occurs within a 15-day period during all ENSO phases for all five groups. The similarity in these dates suggests regional upper-level subsidence and or a marked decrease in regional moisture influx. While Group 5 does have the earliest dry season onset, there was no discernible progression in dry season onset in the station groups as there was with wet season onset. Because wet season onset is earliest in Groups 1 and 2 and dry season onset is similar in all the groups, wet season length is also longest in Groups 1 and 2 (Figure 4).

All groups had on average the earliest wet season onset during El Niño years out of all ENSO phases, although this was only statistically significant in Groups 1 and 2 when

compared with La Niña years (Figure 4). This finding departs from studies (e.g., Francou *et al.*, 2003) that reference the work done on the Zongo Glacier during the 1997–1998 El Niño year by Wagnon *et al.* (2001) to support a delay in the wet season onset during El Niño years. While the mean wet season onset of Group 2, which is nearest the Zongo Glacier, is earlier (10/25) during the 1997–1998 El Niño, three stations from this group during this year had wet season onsets nearly 2 months later. Drops in daily precipitation after the wet season onset during El Niño years (Figure 5) could explain this difference if some stations do not benefit from the brief onset-inducing rains. This is supported by Wagnon *et al.* (2001), who reported through their observations of increased glacial ablation during the 1997–1998 El Niño year that El Niño years associate with more dry periods throughout the wet season, not necessarily at the beginning of the wet season. The increased glacial ablation observed during El Niño might be explained by other mechanisms, such as increased temperature (Ramirez *et al.*, 2001; Francou *et al.*, 2003; Bradley *et al.*, 2006), decreased albedo (Francou *et al.*, 2003), an increased fraction of precipitation falling as rain (Endries *et al.*, 2018; Veettil *et al.*, 2018), or larger spans of sunny days during the wet season (Francou *et al.*, 2003; Favier *et al.*, 2004).

5.5 | Different ENSO flavours

Analysis of the scatterplots of wet season precipitation and January–February MEI values reveals that ENSO events of comparable magnitude do not evoke the same response (Figure 6). For instance, wet season totals in Group 4 vary over 400 mm among the four strongest El Niño events, with totals in the El Niño of 1997–1998 comparable to the four strongest La Niña events. Indeed, multiple recent investigations (Sulca *et al.*, 2018; Imfeld *et al.*, 2019; Huerta and Lavado-Casimiro, 2020) have found varying precipitation responses in southern Peru depending if warmer waters were centred over the Central Tropical Pacific or the Eastern Tropical Pacific (e.g., Indicators Central (C) and Eastern (E) in Takahashi *et al.*, 2011). Although the investigation of the spatiotemporal patterns of precipitation in southern Peru and Bolivia during these different flavours of El Niño was beyond the scope of our study, future research should consider analysing further.

Whereas ENSO phases are forecast months in advance (Climate Prediction Center), the MEI and this study do not distinguish among differing SST patterns (i.e., Indicators C and E in Takahashi *et al.*, 2011) in different Pacific Ocean regions, which limits accurate predictions of precipitation responses to ENSO phases in the western groups. Prediction of precipitation responses by ENSO phase in the eastern groups, however, may be more accurate regardless of which flavour of El Niño persists. The scatterplots in Group 1 and 2 reveal tighter groups of wet season totals among the strongest El Niño and La Niña years.

6 | SUMMARY AND CONCLUSIONS

This paper has explored ENSO-precipitation relationships in the outer tropical Andes of southern Peru and Bolivia. By creating five optimally chosen station groups in the outer tropical Andes of southern Peru and Bolivia, this study uncovered two areas (East and West) with differing precipitation responses to ENSO forcing of regional climate. The groups farthest from the Amazon, (3, 4, and 5, western side of the study area), largely followed the traditional understanding of ENSO-precipitation relationships and recorded fewer wet days, fewer very wet days, negative annual precipitation anomalies, and negative seasonal precipitation anomalies during El Niño years. The eastern groups, nearest to the Amazon and incorporating sites such as the Quelccaya Icecap, Cusco, and La Paz, exhibited the highest wet season and annual precipitation during ENSO Neutral years. During El Niño, these groups produced more wet days, more very wet days, positive annual precipitation anomalies, and positive seasonal precipitation anomalies than in La Niña years, although none of these variables are statistically different. Finally, although some studies (e.g., Francou *et al.*, 2003) suggested wet season onset was delayed during El Niño when compared with ENSO Neutral or La Niña years, this paper demonstrated that wet season onset was earliest during El Niño years and was most delayed during La Niña years in all five station groups. Findings from this study should prove valuable for enhanced interpretation ENSO predictions for subregional precipitation variability across the northern Altiplano and surrounding areas in southern Peru and Bolivia and reinterpretation of ice cores from glaciers such as Quelccaya Icecap located in the eastern cordilleras.

ACKNOWLEDGEMENTS

The authors are grateful to the dedicated professionals of SENAMHI Peru, SENAMHI Bolivia, the DECADE Project, and the ESRL of NOAA for the countless hours of work necessary to observe, formulate, and make available the critical climate data for this paper. This work is supported by funding from the National Science Foundation Grant AGS-1347179 (CAREER: Multiscale Investigations of Tropical Andean Precipitation) to L.B. Perry. Special thanks are also due to Dr. Johnathan Sugg,

Dr. Anton Seimon, Dr. Alice Weldon, and Montana Eck for invaluable advice and feedback, and to partners and other family members for their patience and loving support.

ORCID

L. Baker Perry https://orcid.org/0000-0003-0598-6393

REFERENCES

Aalto, R., Maurice-Bourgoin, L., Dunne, T., Montgomery, D.R., Nittrouer, C.A. and Guyot, J.L. (2003) Episodic sediment accumulation on Amazonian flood plains influenced by El Nino/southern oscillation. *Nature*, 425(6957), 493–497. https://doi.org/10.1038/nature02002.

Aceituno, P. (1988) On the functioning of the southern oscillation in the south American sector. Part I: surface climate. *Monthly Weather Review*, 116(3), 505–524. https://doi.org/10.1175/1520-0493(1988)116<0505:OTFOTS>2.0.CO;2.

Anderson, E.P., Marengo, J., Villalba, R., Halloy, S., Young, B., Cordero, D., Gast, F., Jaimes, E., Ruiz, D., Herzog, S.K. and Martinez, R., 2017. *Consequences of climate change for ecosystems and ecosystem services in the tropical Andes. . INCT-Mudancas Climaticas*. Montivedeo, Uruguay: Inter-American Institute of Global Change Research (IAI).

Andrade, M.F., Moreno, I., Calle, J.M., Ticona, L., Blacutt, L., Lavado-Casimiro, W., Sabino, E., Huerta, A., Aybar, C., Hunziker, S. and Brönnimann, S., 2018. *Atlas-Clima y eventos extremos del Altiplano Central Perú-Boliviano*. Carrasco, La Paz, Bolivia: Imprenta A.G.

Bonferroni, C. (1936) Teoria statistica delle classi e calcolo delle probabilita. *Pubblicazioni del R Istituto Superiore di Scienze Economiche e Commericiali di Firenze*, 8, 3–62.

Bradley, R.S., Vuille, M., Diaz, H.F. and Vergara, W. (2006) Threats to water supplies in the tropical Andes. *Science*, 312(5781), 1755–1756. https://doi.org/10.1126/science.1128087.

Caliński, T. and Harabasz, J. (1974) A dendrite method for cluster analysis. *Communications in Statistics-theory and Methods*, 3 (1), 1–27.

Chavez, S.P. and Takahashi, K. (2017) Orographic rainfall hot spots in the Andes-Amazon transition according to the TRMM precipitation radar and in situ data. *Journal of Geophysical Research-Atmospheres*, 122(11), 5870–5882. https://doi.org/10.1002/2016JD026282.

Climate Prediction Center, 2018. Climate Prediction Center - ONI. Origin.cpc.ncep.noaa.gov. Available at: http://origin.cpc.ncep.noaa.gov/products/analysis_monitoring/ensostuff/ONI_v5.php [Accessed 15 November 2018].

Dunn, O.J. (1964) Multiple comparisons using rank sums. *Technometrics*, 6(3), 241–252.

Eck, M.A., Perry, L.B., Soulé, P.T., Sugg, J.W. and Miller, D.K. (2017) Winter climate variability in the southern Appalachian Mountains, 1910–2017. *International Journal of Climatology*, 39 (1), 206–217. https://doi.org/10.1002/joc.5795.

Endries, J.L., Perry, L.B., Yuter, S.E., Seimon, A., Andrade-Flores, M., Winkelmann, R., Quispe, N., Rado, M., Montoya, N., Velarde, F. and Arias, S. (2018) Radar-observed characteristics of precipitation in the tropical high Andes of southern Peru and Bolivia. *Journal of Applied Meteorology and Climatology*, 57, 1441–1458. https://doi.org/10.1175/JAMC-D-17-0248.1.

Espinoza, J.C., Chavez, S., Ronchail, J., Junquas, C., Takahashi, K. and Lavado, W. (2015) Rainfall hotspots over the southern tropical Andes: spatial distribution, rainfall intensity, and relations with large-scale atmospheric circulation. *Water Resources Research*, 51 (5), 3459–3475. https://doi.org/10.1002/2014WR016273.

Favier, V., Wagnon, P. and Ribstein, P. (2004) Glaciers of the outer and inner tropics: a different behaviour but a common response to climatic forcing. *Geophysical Research Letters*, 31, L16403. https://doi.org/10.1029/2004GL020654.

Figueroa, S.N., Satyamurty, P. and Da Silva Dias, P.L. (1995) Simulations of the summer circulation over the south American region with an eta coordinate model. *Journal of the Atmospheric Sciences*, 52(10), 1573–1584. https://doi.org/10.1175/1520-0469(1995)052<1573:SOTSCO>2.0.CO;2.

Francou, B. and Pizarro, L. (1985) El Nino y la sequía en los altos Andes Centrales. *Bulletin de l'Institut Français D'études Andines*, 14(1–2), 1–18.

Francou, B. and Vincent, C. (2007) *Les Glaciers à L'épreuve Du Climat*. Paris: Editions Belin-IRD, p. 274.

Francou, B., Vuille, M., Wagnon, P., Mendoza, J. and Sicart, J.E. (2003) Tropical climate change recorded by a glacier in the Central Andes during the last decades of the twentieth century: Chacaltaya, Bolivia, 16 S. *Journal of Geophysical Research-Atmospheres*, 108. 4154. https://doi.org/10.1029/2002JD002959.

Garreaud, R. (1999) Cold air incursions over subtropical and tropical South America: a numerical case study. *Monthly Weather Review*, 127(12), 2823–2853. https://doi.org/10.1175/1520-0493(1999)127<2823:CAIOSA>2.0.CO;2.

Garreaud, R. (2000) Cold air incursions over subtropical South America: mean structure and dynamics. *Monthly Weather Review*, 128(7), 2544–2559. https://doi.org/10.1175/1520-0493(2000)128<2544:CAIOSS>2.0.CO;2.

Garreaud, R. and Aceituno, P. (2001) Interannual rainfall variability over the south American Altiplano. *Journal of Climate*, 14(12), 2779–2789.

Garreaud, R., Vuille, M. and Clement, A.C. (2003) The climate of the Altiplano: observed current conditions and mechanisms of past changes. *Palaeogeography, Palaeoclimatology, Palaeoecology*, 194(1–3), 5–22. https://doi.org/10.1175/1520-0442(2001)014<2779:IRVOTS>2.0.CO;2.

Giráldez, L., Silva, Y., Zubieta, R. and Sulca, J. (2020) Change of the rainfall seasonality over central Peruvian Andes: onset, end, duration and its relationship with large-scale atmospheric circulation. *Climate*, 8, 23. https://doi.org/10.3390/cli8020023.

Guy, H., Seimon, A., Perry, L.B., Konecky, B.L., Rado, M., Andrade, M., Potocki, M. and Mayewski, P.A. (2019) Subseasonal variations of stable isotopes in tropical Andean precipitation. *Journal of Hydrometeorology*, 20, 915–933. https://doi.org/10.1175/JHM-D-18-0163.1

Haines, S.A., Mayewski, P.A., Kurbatov, A.V., Maasch, K.A., Sneed, S.B., Spaulding, N.E., Dixon, D.A. and Bohleber, P.D. (2016) Ultra-high resolution snapshots of three multi-decadal periods in an Antarctic ice core. *Journal of Glaciology*, 62(231), 31–36. https://doi.org/10.1017/jog.2016.5.

Hartigan, J.A. and Wong, M.A. (1979) Algorithm AS 136: a k-means clustering algorithm. *Journal of the Royal Statistical Society: Series C: Applied Statistics*, 28(1), 100–108.

Heidinger, H., Carvalho, L., Jones, C., Posadas, A. and Quiroz, R. (2018) A new assessment in total and extreme rainfall trends over central and southern Peruvian Andes during 1965–2010. *International Journal of Climatology*, 38, e998–e1015. https://doi.org/10.1002/joc.5427.

Huerta, A. and Lavado-Casimiro, W. (2020) Trends and variability of precipitation extremes in the Peruvian Altiplano (1971–2013). *International Journal of Climatology*, 41, 1–16. https://doi.org/10.1002/joc.6635.

Hunziker, S., Brönnimann, S., Calle, J., Moreno, I., Andrade, M., Ticona, L., Huerta, A. and Lavado-Casimiro, W. (2018) Effects of undetected data quality issues on climatological analyses. *Climate of the Past*, 14(1), 1–20. https://doi.org/10.5194/cp-14-1-2018.

Imfeld, N., Barreto Schuler, C., Correa Marrou, K.M., Jacques-Coper, M., Sedlmeier, K., Gubler, S., Huerta, A. and Brönnimann, S. (2019) Summertime precipitation deficits in the southern Peruvian highlands since 1964. *International Journal of Climatology*, 39(11), 4497–4513. https://doi.org/10.1002/joc.6087.

Imfeld, N., Sedlmeier, K., Gubler, S., Correa Marrou, K., Davila, C.P., Huerta, A., Lavado-Casimiro, W., Rohrer, M., Scherrer, S.C. and Schwierz, C. (2021) A combined view on precipitation and temperature climatology and trends in the southern Andes of Peru. *Int J Climatol*, 41, 679–698. https://doi.org/10.1002/joc.6645.

Junquas, C., Takahashi, K., Condom, T., Espinoza, J.C., Chavez, S., Sicart, J.E. and Lebel, T. (2018) Understanding the influence of orography on the precipitation diurnal cycle and the associated atmospheric processes in the Central Andes. *Climate Dynamics*, 50(11–12), 3995–4017. https://doi.org/10.1007/s00382-017-3858-8.

Knüsel, S., Brütsch, S., Henderson, K.A., Palmer, A.S. and Schwikowski, M. (2005) ENSO signals of the twentieth century in an ice core from Nevado Illimani, Bolivia. *Journal of Geophysical Research-Atmospheres*, 110. D01102https://doi.org/10.1029/2004JD005420.

Kruskal, W.H. and Wallis, W.A. (1952) Use of ranks in one-criterion variance analysis. *Journal of the American Statistical Association*, 47(260), 583–621.

Lenters, J.D. and Cook, K.H. (1999) Summertime precipitation variability over south america: role of the large-scale circulation, *Monthly Weather Review*, 127(3), 409–431. https://doi.org/10.1175/1520-0493(1999)127<0409:SPVOSA>2.0.CO;2

Liebmann, B., Camargo, S.J., Seth, A., Marengo, J.A., Carvalho, L. M., Allured, D., Fu, R. and Vera, C.S. (2007) Onset and end of the rainy season in South America in observations and the ECHAM 4.5 atmospheric general circulation model. *Journal of Climate*, 20(10), 2037–2050. https://doi.org/10.1175/JCLI4122.1.

López-Moreno, J.I., Fontaneda, S., Bazo, J., Revuelto, J., Azorin-Molina, C., Valero-Garcés, B., Morán-Tejeda, E., Cincente-Serrano, S.M., Zubeita, R. and Alejo-Cochachín, J. (2014) Recent glacier retreat and climate trends in cordillera Huaytapallana, Peru. *Global and Planetary Change*, 112, 1–11. https://doi.org/10.1016/j.gloplacha.2013.10.010.

Maussion, F., Gurgiser, M., Großhauser, M., Kaser, G. and Marzeion, B. (2015) ENSO influence on surface energy and mass balance at Shallap glacier, cordillera Blanca, Peru. *The Cryosphere*, 9, 1633–1683. https://doi.org/10.5194/tc-9-1663-2015.

Perry, L.B., Seimon, A., Andrade-Flores, M.F., Endries, J.L., Yuter, S.E., Velarde, F., Arias, S., Bonshoms, M., Burton, E.J., Winkelmann, I.R. and Cooper, C.M. (2017) Characteristics of precipitating storms in glacierized tropical Andean cordilleras of Peru and Bolivia. *Annals of the American Association of Geographers*, 107(2), 309–322. https://doi.org/10.1080/24694452.2016.1260439.

Perry, L.B., Seimon, A. and Kelly, G.M. (2014) Precipitation delivery in the tropical high Andes of southern Peru: new findings and paleoclimatic implications. *International Journal of Climatology*, 34(1), 97–215. https://doi.org/10.1002/joc.3679.

Philander, S.G.H. (1983) El Nino southern oscillation phenomena. *Nature*, 302(5906), 295–301. https://doi.org/10.1038/302295a0.

Rabatel, A., Francou, B., Soruco, A., Gomez, J., Cáceres, B., Ceballos, J.L., Basantes, R., Vuille, M., Sicart, J.E., Huggel, C. and Scheel, M. (2012) Current state of glaciers in the tropical Andes: a multi-century perspective on glacier evolution and climate change. *The Cryosphere*, 7(1), 81–102. https://doi.org/10.5194/tc-7-81-2013.

Ramirez, E., Francou, B., Ribstein, P., Descloitres, M., Guerin, R., Mendoza, J., Gallaire, R., Pouyaud, B. and Jordan, E. (2001) Small glaciers disappearing in the tropical Andes: a case-study in Bolivia: Glaciar Chacaltaya (16 S). *Journal of Glaciology*, 47(157), 187–194. https://doi.org/10.3189/172756501781832214.

Ramirez, E., Hoffmann, G., Taupin, J.D., Francou, B., Ribstein, P., Caillon, N., Ferron, F.A., Landais, A., Petit, J.R., Pouyaud, B. and Schotterer, U. (2003) A new Andean deep ice core from Nevado Illimani (6350 m), Bolivia. *Earth and Planetary Science Letters*, 212(3–4), 337–350. https://doi.org/10.1016/S0012-821X(03)00240-1.

Ribstein, P., Tiriau, E., Francou, B. and Saravia, R. (1995) Tropical climate and glacier hydrology: a case study in Bolivia. *Journal of Hydrology*, 165(1–4), 221–234. https://doi.org/10.1016/0022-1694(94)02572-S.

Rodwell, M.J. and Hoskins, B.J. (2001) Subtropical anticyclones and summer monsoons. *Journal of Climate*, 14(15), 3192–3211. https://doi.org/10.1175/1520-0442(2001)014<3192:SAASM>2.0.CO;2.

Ronchail, J. and Gallaire, R. (2006) ENSO and rainfall along the Zongo valley (Bolivia) from the Altiplano to the Amazon basin. *International Journal of Climatology*, 26(9), 1223–1236. https://doi.org/10.1002/joc.1296.

Seluchi, M.E., Saulo, A.C., Nicolini, M. and Satyamurty, P. (2003) The northwestern Argentinean low: a study of two typical events. *Monthly Weather Review*, 131(10), 2361–2378. https://doi.org/10.1175/1520-0493(2003)131<2361:TNALAS>2.0.CO;2.

Soruco, A., Vincent, C., Francou, B. and Gonzalez, J.F. (2009) Glacier decline between 1963 and 2006 in the cordillera real, Bolivia. *Geophysical Research Letters*, 36. L03502. https://doi.org/10.1029/2008GL036238.

Sulca, J., Takahashi, K., Espinoza, J.C., Vuille, M. and Lavado-Casimiro, W. (2018) Impacts of different ENSO flavors and tropical Pacific convection variability (ITCZ, SPCZ) on austral summer rainfall in South America, with a focus on Peru. *International Journal of Climatology*, 38(1), 420–435. https://doi.org/10.1002/joc.5185.

Takahashi, K., Montecinos, A., Goubanova, K. and Dewitte, B. (2011) ENSO regimes: reinterpreting the canonical and Modoki

El Niño. *Geophysical Research Letters*, 38, L10704. https://doi.org/10.1029/2011GL047364.

Thompson, L.G., Mosley-Thompson, E., Dansgaard, W. and Grootes, P.M. (1986) The little ice age as recorded in the stratigraphy of the tropical Quelccaya ice cap. *Science*, 234(4774), 361–364. https://doi.org/10.1126/science.234.4774.361.

Trenberth, K.E. (1997) The definition of El Niño. *Bulletin of the American Meteorological Society*, 78(12), 2771–2778. https://doi.org/10.1175/1520-0477(1997)078<2771:TDOENO>2.0.CO;2.

Urrutia, R. and Vuille, M. (2009) Climate change projections for the tropical Andes using a regional climate model: temperature and precipitation simulations for the end of the 21st century. *Journal of Geophysical Research-Atmospheres*, 114. D02108. https://doi.org/10.1029/2008JD011021.

Veettil, B.K., Bremer, U.F., de Souza, S.F., Maier, É.L.B. and Simões, J.C. (2016) Influence of ENSO and PDO on mountain glaciers in the outer tropics: case studies in Bolivia. *Theoretical and Applied Climatology*, 125(3–4), 757–768. https://doi.org/10.1007/s00704-015-1545-4.

Veettil, B.K., Wang, S., Simões, J.C., Ruiz Pereira, S.F. and de Souza, S.F. (2018) Regional climate forcing and topographic influence on glacier shrinkage: eastern cordilleras of Peru. *International Journal of Climatology*, 38, 979–995. https://doi.org/10.1002/joc.5226.

Vimeux, F., Gallaire, R., Bony, S., Hoffmann, G. and Chiang, J.C. (2005) What are the climate controls on δD in precipitation in the Zongo Valley (Bolivia)? Implications for the Illimani ice core interpretation. *Earth and Planetary Science Letters*, 240(2), 205–220. https://doi.org/10.1016/j.epsl.2005.09.031.

Vuille, M. (1999) Atmospheric circulation over the Bolivian Altiplano during dry and wet periods and extreme phases of the southern oscillation. *International Journal of Climatology*, 19 (14), 1579–1600.

Vuille, M., Bradley, R.S. and Keimig, F. (2000) Interannual climate variability in the Central Andes and its relation to tropical Pacific and Atlantic forcing. *Journal of Geophysical Research-Atmospheres*, 105(D10), 12447–12460. https://doi.org/10.1029/2000JD900134.

Vuille, M., Carey, M., Huggel, C., Buytaert, W., Rabatel, A., Jacobsen, D., Soruco, A., Villacis, M., Yarleque, C., Timm, O.E. and Condom, T. (2017) Rapid decline of snow and ice in the tropical Andes–impacts, uncertainties and challenges ahead. *Earth-Science Reviews*, 176, 195–213. https://doi.org/10.1016/j.earscirev.2017.09.019.

Vuille, M., Hardy, D.R., Braun, C., Keimig, F. and Bradley, R.S. (1998) Atmospheric circulation anomalies associated with 1996/1997 summer precipitation events on Sajama ice cap, Bolivia. *Journal of Geophysical Research-Atmospheres*, 103 (D10), 11191–11204. https://doi.org/10.1029/98JD00681.

Wagnon, P., Ribstein, P., Francou, B. and Sicart, J.E. (2001) Anomalous heat and mass budget of Glaciar Zongo, Bolivia, during the 1997/98 El Niño year. *Journal of Glaciology*, 47(156), 21–28. https://doi.org/10.3189/172756501781832593.

How to cite this article: Jonaitis JA, Perry LB, Soulé PT, *et al.* Spatiotemporal patterns of ENSO-precipitation relationships in the tropical Andes of southern Peru and Bolivia. *Int J Climatol*. 2021;1–16. https://doi.org/10.1002/joc.7058